

# Phase Structure in a Hadronic Chiral Model

D. Zschesche<sup>a</sup>, G. Zeeb<sup>a</sup> and S. Schramm<sup>a,b</sup>

<sup>a</sup>*Institut für Theoretische Physik, J. W. Goethe-Universität,  
Max-von-Laue-Str. 1, 60438 Frankfurt, Germany and*

<sup>b</sup>*Center for Scientific Computing (CSC), J. W. Goethe-Universität,  
Max-von-Laue-Str. 1, 60438 Frankfurt, Germany*

(Dated: February 9, 2008)

We study the phase diagram of a hadronic chiral flavor- $SU(3)$  model. Heavy baryon resonances can induce a phase structure that matches current results from lattice-QCD calculations at finite temperature and baryon density. Furthermore, we determine trajectories of constant entropy per net baryon in the phase diagram.

Understanding hot and baryon-dense QCD matter is of central importance in theoretical and experimental heavy-ion physics. Various effective theories for chiral symmetry restoration predict that a line of first-order phase transitions in the plane of quark-chemical potential  $\mu_q$  versus temperature  $T$  ends in a critical point as the chemical potential is lowered (see [1] for a review). Presently, the lattice locates that point at  $T \approx 160$  MeV,  $\mu_q \approx 120$  MeV [2]. The Compressed Baryonic Matter (CBM) experiment at GSI FAIR is planned to perform a dedicated experimental effort to detect that line of first-order phase transitions in relativistic heavy-ion collisions. It is hoped that by varying experimental parameters like the beam energy one could trigger phase transitions of variable strength (latent heat) and perhaps even locate the expected second-order critical point.

Models relying exclusively on order-parameter dynamics typically predict significantly lower chiral phase transition temperatures in baryon-dense matter than those found on the lattice (see e.g. Fig. 6 in [1]). As shown by Gerber and Leutwyler some time ago [3], while heavy hadronic states are suppressed by the Boltzmann factor, their contribution to the energy density at high temperature is substantial. This agrees with other studies using a hadron resonance gas approach, which provides a reasonable description of the thermodynamics obtained on the lattice below the critical temperature [4]. Heavy states also reduce [3] the strong dependence of the “critical temperature” (defined via the peak of a suitable susceptibility) on the pion mass obtained in simple models for chiral order parameter dynamics [5]. The lattice indicates a relatively weak dependence of  $T_c$  on the pion mass [6].

In this Letter we investigate the role of heavy hadronic states on the location of the chiral critical point within a non-linear  $SU(3)_L \times SU(3)_R$  chiral model [7]. Here, the phase transition at high temperature and baryon density is “driven” by baryonic resonance degrees of freedom, as suggested by the discussion above. We shall show that the model is able to reproduce not only the sketched qualitative phase structure but also the location of the endpoint. The properties of the high mass states (masses and couplings) are important for the actual location of

the chiral phase transition line [8] in the plane of  $T$  and  $\mu_q$ .

Lattice results show that the susceptibility peaks of the chiral condensate and of the Polyakov loop coincide at  $\mu_q = 0$  [9] which indicates that for small  $\mu_q$  those transition(s) involve a coupling of the chiral dynamics to the gauge fields, see e.g. [10]. However, within a matrix model for Polyakov loops, the effect of  $\mu_q > 0$  on the critical temperature for deconfinement is suppressed by  $1/N_c$  [11]. In contrast,  $\mu$ -effects on the chiral critical temperature could be relatively strong. Indeed, models which couple chiral fields to Polyakov loops do suggest a decoupling of chiral and deconfinement dynamics at large chemical potential, and that the largest increase in the Polyakov loop still appears at  $T \approx T_c(\mu = 0)$ , while the peak of the chiral susceptibility is shifted to significantly smaller  $T$  [10]. Thus at large chemical potential a confined phase with partially restored chiral symmetry might exist.

Our chiral hadronic  $SU(3)$  Lagrangian incorporates the complete set of baryons from the lowest flavor- $SU(3)$  octet, as well as the entire multiplets of scalar, pseudoscalar, vector and axialvector mesons [7, 12]. In mean-field approximation, the expectation values of the scalar fields relevant for symmetric nuclear matter correspond to the non-strange and strange chiral quark condensates, namely the  $\sigma$  and its  $s\bar{s}$  counterpart  $\zeta$ , respectively, and further the  $\omega$  and  $\phi$  vector meson fields. Another scalar isoscalar field, the dilaton  $\chi$ , is introduced to model the QCD scale anomaly. However, if  $\chi$  does not couple strongly to baryonic degrees of freedom then it remains essentially “frozen” below the chiral transition. Consequently, we focus here on the role of the quark condensates.

Interactions between baryons and scalar (BM) or vector (BV) mesons, respectively, are introduced as

$$\mathcal{L}_{\text{BM}} = - \sum_i \bar{\psi}_i (g_{i\sigma}\sigma + g_{i\zeta}\zeta) \psi_i, \quad (1)$$

$$\mathcal{L}_{\text{BV}} = - \sum_i \bar{\psi}_i (g_{i\omega}\gamma_0\omega^0 + g_{i\phi}\gamma_0\phi^0) \psi_i, \quad (2)$$

Here,  $i$  sums over the baryon octet ( $N, \Lambda, \Sigma, \Xi$ ). A term  $\mathcal{L}_{\text{vec}}$  with mass terms and quartic self-interaction of the

vector mesons is also added:

$$\mathcal{L}_{\text{vec}} = \frac{1}{2}a_\omega\chi^2\omega^2 + \frac{1}{2}a_\phi\chi^2\phi^2 + g_4^4(\omega^4 + 2\phi^4).$$

The scalar self-interactions are

$$\begin{aligned} \mathcal{L}_0 = & -\frac{1}{2}k_0\chi^2(\sigma^2 + \zeta^2) + k_1(\sigma^2 + \zeta^2)^2 + k_2\left(\frac{\sigma^4}{2} + \zeta^4\right) \\ & + k_3\chi\sigma^2\zeta - k_4\chi^4 - \frac{1}{4}\chi^4\ln\frac{\chi^4}{\chi_0^4} + \frac{\delta}{3}\chi^4\ln\frac{\sigma^2\zeta}{\sigma_0^2\zeta_0} \end{aligned} \quad (3)$$

Interactions between the scalar mesons induce the spontaneous breaking of chiral symmetry (first line) and the scale breaking via the dilaton field  $\chi$  (last two terms).

Non-zero current quark masses break chiral symmetry explicitly in QCD. In the effective Lagrangian this corresponds to terms such as

$$\mathcal{L}_{\text{SB}} = -\frac{\chi^2}{\chi_0^2} \left[ m_\pi^2 f_\pi \sigma + (\sqrt{2}m_K^2 f_K - \frac{1}{\sqrt{2}}m_\pi^2 f_\pi) \zeta \right] \quad (4)$$

According to  $\mathcal{L}_{\text{BM}}$  (1), the effective masses of the baryons,  $m_i^*(\sigma, \zeta) = g_{i\sigma}\sigma + g_{i\zeta}\zeta$ , are generated through their coupling to the chiral condensates, which attain non-zero vacuum expectation values due to their self-interactions [7] in  $\mathcal{L}_0$  (3). The effective masses of the mesons are obtained as the second derivatives of the mesonic potential about its minimum.

The baryon-vector couplings  $g_{i\omega}$  and  $g_{i\phi}$  result from pure  $f$ -type coupling as discussed in [7],  $g_{i\omega} = (n_q^i - n_{\bar{q}}^i)g_8^V$ ,  $g_{i\phi} = -(n_s^i - n_{\bar{s}}^i)\sqrt{2}g_8^V$ , where  $g_8^V$  denotes the vector coupling of the baryon octet and  $n^i$  the number of constituent quarks of species  $i$  in a given hadron. The resulting relative couplings agree with additive quark model constraints.

All parameters of the model discussed so far are fixed by either symmetry relations, hadronic vacuum observables or nuclear matter saturation properties (for details see [7]). In addition, the model also provides a satisfactory description of realistic (finite-size and isospin asymmetric) nuclei and of neutron stars [7, 13].

If the baryonic degrees of freedom are restricted to the members of the lowest lying octet, the model exhibits a smooth decrease of the chiral condensates (crossover) for both high  $T$  and high  $\mu$  [7, 12]. However, additional baryonic degrees of freedom may change this into a first-order phase transition in certain regimes of the  $T$ - $\mu_q$  plane, depending on the couplings [8, 12, 14]. To model the influence of such heavy baryonic states, we add a single resonance with mass  $m_R = m_0 + g_R\sigma$  and vector coupling  $g_{R\omega} = r_V g_{N\omega}$ . The mass parameters,  $m_0$ ,  $g_R$  and the relative vector coupling  $r_V$  represent free parameters, adjusted to reproduce the phase diagram discussed above [19]. In principle, of course, one should include the entire spectrum of resonances. However, to keep the number of additional couplings small, we effectively describe all higher baryonic resonances by a single state with adjustable couplings, mass and degeneracy.

In what follows, the meson fields are replaced by their (classical) expectation values, which corresponds to neglecting quantum and thermal fluctuations. Fermions, of course, have to be integrated out to one-loop. The grand canonical potential can then be written as

$$\begin{aligned} \Omega/V = & -\mathcal{L}_{\text{vec}} - \mathcal{L}_0 - \mathcal{L}_{\text{SB}} - \mathcal{V}_{\text{vac}} \\ & - T \sum_{i \in B} \frac{\gamma_i}{(2\pi)^3} \int d^3k \left[ \ln \left( 1 + e^{-\frac{1}{T}[E_i^*(k) - \mu_i^*]} \right) \right] \\ & + T \sum_{l \in M} \frac{\gamma_l}{(2\pi)^3} \int d^3k \left[ \ln \left( 1 - e^{-\frac{1}{T}[E_l^*(k) - \mu_l^*]} \right) \right], \end{aligned} \quad (5)$$

where  $\gamma_B, \gamma_M$  denote the baryonic and mesonic spin-isospin degeneracy factors, respectively, and  $E_{B,M}^*(k) = \sqrt{k^2 + m_{B,M}^{*2}}$  are the corresponding single particle energies. In the second line we sum over the baryon octet states plus the additional heavy resonance with degeneracy  $n$  (assumed to be 16). The effective baryon-chemical potentials are  $\mu_i^* = \mu_i - g_{i\omega}\omega - g_{i\phi}\phi$ , with  $\mu_i = (n_q^i - n_{\bar{q}}^i)\mu_q + (n_s^i - n_{\bar{s}}^i)\mu_s$ . The chemical potentials of the mesons are given by the sum of the corresponding quark and anti-quark chemical potentials. The vacuum energy  $\mathcal{V}_{\text{vac}}$  (the potential at  $\rho_B = T = 0$ ) has been subtracted.

By extremizing  $\Omega/V$  one obtains self-consistent gap equations for the mesons. Here, we consider non-strange matter, adjusting  $\mu_s$  for any given  $T$  and  $\mu_q$  so that the net number of strange quarks is zero. The dominant “condensates” then are the  $\sigma$  and the  $\omega$  fields.

The properties of the QCD transition at vanishing chemical potential depend on the number of quark flavors and on their masses. In quenched lattice gauge theory, which corresponds to infinitely heavy quarks, the critical temperature is  $T_c \approx 260$  MeV [15]. Smaller quark or pion masses, respectively, reduce the critical temperature [6]. Lattice calculations with 2 and 3 flavors of light quarks predict critical temperatures of  $T_c \approx 175$  MeV and  $T_c \approx 155$  MeV, respectively. However, we note that recently [16] values as high as 190 MeV were reported for the 2-flavor case with reasonably small quark masses, and for reduced pion over-degeneracy on the lattice. For two flavors, the lattice results support a continuous transition in agreement with symmetry arguments [15]. For three massless flavors, a first-order phase transition is expected, which is washed out at a pion mass of  $m_\pi \approx 70 - 260$  MeV [15].

Within our model, at zero baryon density we obtain values for the critical temperature around 140–190 MeV, which are in reasonable agreement with the numbers obtained from lattice calculations. Furthermore, we observe a rather slow increase of the critical temperature with increasing explicit mass term  $m_0$  (corresponding to the quark mass term of QCD, cf. Fig. 1). Finally, the first-order phase transition observed for small explicit mass term indeed turns into a crossover beyond some criti-

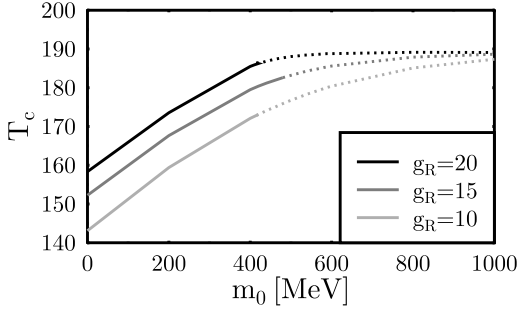


FIG. 1: Critical temperature  $T_c$  at vanishing chemical potential vs the explicit mass term  $m_0$  for different values of the scalar coupling  $g_R$ . Full lines denote a first-order phase transition and dotted lines correspond to a crossover.

cal value of  $m_0$ . Neglecting the octet hyperons, which basically corresponds to the two-flavor limit, leaves a crossover at  $\mu = 0$  and increases the critical temperature. If in turn we assign the additional resonance to a spin-3/2 decuplet of flavor- $SU(3)$  and take the 3-flavor limit then chiral restoration happens via a first-order phase transition and the critical temperature drops by  $\approx 30$  MeV. This behavior is also in (qualitative) agreement with the lattice QCD findings described above.

We now turn to non-zero (net) baryon density. Within certain ranges for the mass and couplings of the heavy resonance, the location of the critical endpoint is reasonably close to the lattice results. This is in contrast to models which do not account for heavy degrees of freedom and usually predict the endpoint at too low temperature (see e.g. [1] for a summary). Choosing, for example,  $m_R(\sigma_0) = 2$  GeV,  $r_V = 0.4$  and  $m_0 = 0.57$  GeV results in  $T_E \approx 180$  MeV (see Fig. 2). This is a little higher than  $T_E$  from Ref. [2] but the peak of the susceptibility of the order parameter at  $\mu = 0$  is at  $T_c = 185.6$  MeV, in good agreement with the recent lattice results at zero density. Smaller explicit mass term  $\sim m_0$  for the additional heavy resonance moves the critical endpoint closer to the temperature axis, finally turning the crossover at  $\mu_q = 0$  into a first-order transition (cf. Fig. 1) if  $m_0$  drops below a critical value. We also point out that the phase transition at  $T = 0$  occurs at a density above the nuclear matter saturation point, as it should be.

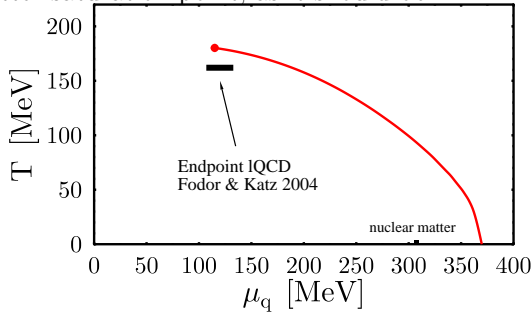


FIG. 2: First-order phase transition line in the  $T$ - $\mu$  plane.  $m_R(\sigma_0) = 2$  GeV,  $r_V = 0.4$  and  $m_0 = 0.57$  GeV.

Figure 3 shows the density and entropy contributions to the latent heat along the transition line of Fig. 2. The latent heat first grows with increasing chemical potential. However, around  $\mu_q \approx 150$  MeV it decreases again, exhibiting a local minimum at  $\mu_q \approx 200$  MeV before in-

creasing again towards low temperature. This structure is also present in the entropy contribution. The density contribution to the latent heat up to  $\mu_q \approx 200$  MeV is flat but then rises very rapidly with increasing chemical potential.

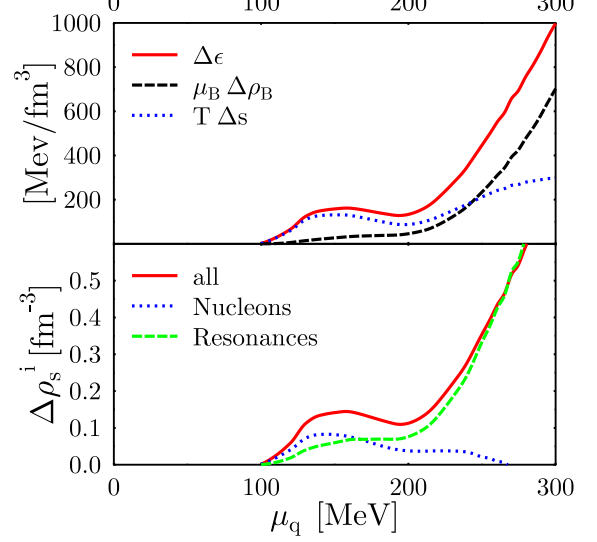


FIG. 3: Top: Latent heat and its entropy ( $T\Delta s$ ) and density ( $\mu_B \Delta \rho_B$ ) contributions along the phase transition line versus the quark chemical potential. Bottom: Difference of the scalar density ( $\Delta \rho_s^i$ ) in the two phases at the phase transition versus the quark chemical potential.

This somehow unexpected behaviour is due to a change in the dominant degrees of freedom. Around  $\mu_q \approx 100 - 150$  MeV nucleons dominate the discontinuity of the scalar density (cf. Fig. 3) at the phase boundary, but this contribution decreases above  $\mu_q \approx 150$  MeV and finally vanishes at  $\mu_q \approx 270$  MeV. In contrast, the contribution of the resonances increases sharply around 200 MeV. Both effects together generate the small dip in the latent heat and the 'nose' in the  $e$ - $\rho_B$  phase diagram, cf. Fig. 5. This behaviour is actually not that surprising given that lattice results at  $\mu_q \approx 0$  suggest just one single peak in all susceptibilities. In contrast, at zero temperature the jump from zero to finite nucleon density signals the liquid-gas phase transition while the chiral transition is expected to happen at larger chemical potential [17], driven by newly populated heavier degrees of freedom.

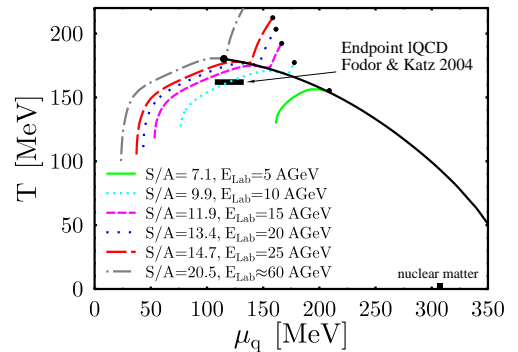


FIG. 4: Phase transition line and adiabats in the  $T$ - $\mu_q$  phase diagram.

Figure 4 depicts lines of constant entropy per net baryon (adiabats) in the phase diagram. These correspond to perfect-fluid expansion trajectories. At the phase transition they “bend” slightly towards smaller chemical potential. For the present EoS, the  $S/A \approx 20$  adiabat goes right through the endpoint of first-order transitions, higher specific entropies then correspond to crossovers. To make contact with experiments, e.g. at

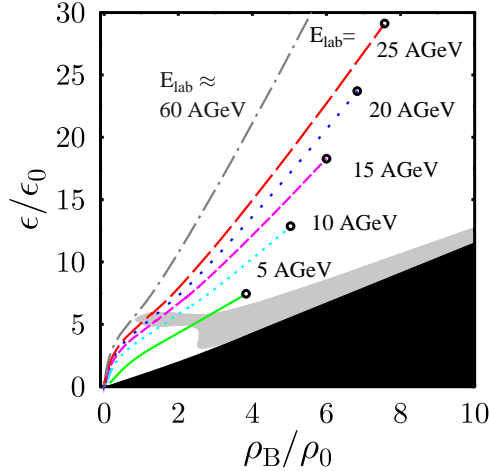


FIG. 5: Adiabats in the  $e$ - $\rho_B$  phase diagram. The grey area represents the mixed phase.

the upcoming GSI-FAIR facility, we use a simple estimate for the initial baryon number and energy density:  $\rho_B^{ini} = 2\gamma_{CM}\rho_0$ ,  $e^{ini} = \sqrt{s}\rho_0\gamma_{CM}$ . This assumes that the entire initial beam energy and baryon number equilibrates in a Lorentz-contracted volume determined by the overlap of projectile and target in the center-of-mass frame. In the energy range of interest here, this simple model reproduces the specific entropy from more realistic three-fluid models quite well [18]. Within this simple model beam energies between 5-10 A GeV are sufficient to overshoot the shaded phase coexistence region (Fig. 5). In the energy range from 5-25 A GeV, adiabatic expansion leads to a first-order phase transition back to the symmetry broken state with a latent heat of  $\approx 120 - 160$  MeV/fm<sup>3</sup>. Higher collision energies lead to weaker (more “critical”) first order transitions. The critical end point of the line of first-order transitions is reached for a beam energy of about 60 AGeV, with higher energies leading to crossover transitions.

In summary, we have explored the influence of heavy baryon resonances on the phase diagram of a flavor- $SU(3)$  hadronic chiral Lagrangian. We find that, with appropriate couplings, the model is able to reproduce

the structure of the QCD phase diagram at finite density in that a line of first-order phase transitions at high density terminates in a critical point at  $T_E \approx 180$  MeV,  $\mu_E \approx 110$  MeV. The interplay of nucleon and resonance contributions to the density may lead to a non-monotonic latent heat along the phase boundary.

We thank A. Dumitru and H. Stöcker for useful discussions. This work was supported by DFG, GSI and BMBF and used computational resources provided by the CSC at the University of Frankfurt, Germany.

- 
- [1] M. A. Stephanov, Prog. Theor. Phys. Suppl. **153** (2004) 139 [Int. J. Mod. Phys. A **20** (2005) 4387].
  - [2] Z. Fodor and S. D. Katz, JHEP **0404** (2004) 050.
  - [3] P. Gerber and H. Leutwyler, Nucl. Phys. B **321** (1989) 387.
  - [4] F. Karsch, K. Redlich and A. Tawfik, Phys. Lett. B **571** (2003) 67.
  - [5] A. Dumitru, D. Roder and J. Ruppert, Phys. Rev. D **70** (2004) 074001.
  - [6] F. Karsch, E. Laermann and A. Peikert, Nucl. Phys. B **605** (2001) 579.
  - [7] P. Papazoglou, D. Zschesche, S. Schramm, J. Schaffner-Bielich, H. Stoecker and W. Greiner, Phys. Rev. C **59** (1999) 411.
  - [8] D. Zschesche, G. Zeeb, S. Schramm and H. Stoecker, J. Phys. G **31**, 935 (2005).
  - [9] F. Karsch, Lect. Notes Phys. **583** (2002) 209.
  - [10] C. Ratti, M. A. Thaler and W. Weise, Phys. Rev. D **73** (2006) 014019.
  - [11] A. Dumitru, R. D. Pisarski and D. Zschesche, Phys. Rev. D **72** (2005) 065008.
  - [12] D. Zschesche, S. Schramm, H. Stoecker and W. Greiner, Phys. Rev. C **65** (2002) 064902.
  - [13] S. Schramm, Phys. Lett. B **560** (2003) 164; S. Schramm, Phys. Rev. C **66** (2002) 064310.
  - [14] J. Theis, G. Graebner, G. Buchwald, J. A. Maruhn, W. Greiner, H. Stoecker and J. Polonyi, Phys. Rev. D **28** (1983) 2286.
  - [15] E. Laermann and O. Philipsen, Ann. Rev. Nucl. Part. Sci. **53** (2003) 163.
  - [16] S. D. Katz, Talk given at Quark Matter 2005.
  - [17] M. A. Halasz, A. D. Jackson, R. E. Shrock, M. A. Stephanov and J. J. M. Verbaarschot, Phys. Rev. D **58** (1998) 096007.
  - [18] M. Reiter *et al.*, Nucl. Phys. A **643** (1998) 99; Y. B. Ivanov, V. N. Russkikh and V. D. Toneev, arXiv:nucl-th/0503088.
  - [19] Note that instead of an explicit mass term we could have coupled the resonance to the dilaton  $\chi$ .